

## Article

# A novel long-term intravenous combined with local treatment with human amnion-derived mesenchymal stem cells for a multidisciplinary rescued uremic calciphylaxis patient and the underlying mechanism

Lianju Qin<sup>1,†,\*</sup>, Jing Zhang<sup>2,†</sup>, Yujie Xiao<sup>2,†</sup>, Kang Liu<sup>2</sup>, Yugui Cui<sup>1</sup>, Fangyan Xu<sup>2</sup>, Wenkai Ren<sup>2</sup>, Yanggang Yuan<sup>2</sup>, Chunyan Jiang<sup>1</sup>, Song Ning<sup>1</sup>, Xiaoxue Ye<sup>2</sup>, Ming Zeng<sup>2</sup>, Hanyang Qian<sup>2</sup>, Anning Bian<sup>2</sup>, Fan Li<sup>2</sup>, Guang Yang<sup>2</sup>, Shaowen Tang<sup>3</sup>, Zhihong Zhang<sup>4</sup>, Juncheng Dai<sup>3</sup>, Jing Guo<sup>5</sup>, Qiang Wang<sup>6</sup>, Bin Sun<sup>2</sup>, Yifei Ge<sup>2</sup>, Chun Ouyang<sup>2</sup>, Xueqiang Xu<sup>2</sup>, Jing Wang<sup>2</sup>, Yaoyu Huang<sup>2</sup>, Hongqing Cui<sup>2</sup>, Jing Zhou<sup>1</sup>, Meilian Wang<sup>7</sup>, Zhonglan Su<sup>8</sup>, Yan Lu<sup>8</sup>, Di Wu<sup>8</sup>, Jingping Shi<sup>9</sup>, Wei Liu<sup>10</sup>, Li Dong<sup>11</sup>, Yinbing Pan<sup>12</sup>, Baiqiao Zhao<sup>2,13</sup>, Ying Cui<sup>2,14</sup>, Xueyan Gao<sup>2,15</sup>, Zhanhui Gao<sup>2,16</sup>, Xiang Ma<sup>1</sup>, Aiqin Chen<sup>1</sup>, Jie Wang<sup>1</sup>, Meng Cao<sup>1</sup>, Qian Cui<sup>1</sup>, Li Chen<sup>1</sup>, Feng Chen<sup>17</sup>, Youjia Yu<sup>17</sup>, Qiang Ji<sup>17</sup>, Zhiwei Zhang<sup>17</sup>, Mufeng Gu<sup>18</sup>, Xiaojun Zhuang<sup>18</sup>, Xiaolin Lv<sup>2</sup>, Hui Wang<sup>2</sup>, Yanyan Pan<sup>2</sup>, Ling Wang<sup>2</sup>, Xianrong Xu<sup>2</sup>, Jing Zhao<sup>19</sup>, Xiuqin Wang<sup>20</sup>, Cuiping Liu<sup>21</sup>, Ningxia Liang<sup>22</sup>, Changying Xing<sup>2</sup>, Jiayin Liu<sup>1,\*</sup>, and Ningning Wang<sup>6,2,\*</sup>

<sup>1</sup> State Key Laboratory of Reproductive Medicine, Center of Clinical Reproductive Medicine, The First Affiliated Hospital of Nanjing Medical University, Jiangsu Province Hospital, Nanjing 210029, China

<sup>2</sup> Department of Nephrology, The First Affiliated Hospital of Nanjing Medical University, Jiangsu Province Hospital, Nanjing 210029, China

<sup>3</sup> Department of Epidemiology and Biostatistics, School of Public Health, Nanjing Medical University, Nanjing 211166, China

<sup>4</sup> Department of Pathology, The First Affiliated Hospital of Nanjing Medical University, Jiangsu Province Hospital, Nanjing 210029, China

<sup>5</sup> Department of Cardiology, The First Affiliated Hospital of Nanjing Medical University, Jiangsu Province Hospital, Nanjing 210029, China

<sup>6</sup> Department of Rheumatology, The First Affiliated Hospital of Nanjing Medical University, Jiangsu Province Hospital, Nanjing 210029, China

<sup>7</sup> Department of Obstetrics, The First Affiliated Hospital of Nanjing Medical University, Jiangsu Province Hospital, Nanjing 210029, China

<sup>8</sup> Department of Dermatology, The First Affiliated Hospital of Nanjing Medical University, Jiangsu Province Hospital, Nanjing 210029, China

<sup>9</sup> Department of Burn and Plastic Surgery, The First Affiliated Hospital of Nanjing Medical University, Jiangsu Province Hospital, Nanjing 210029, China

<sup>10</sup> Department of Nuclear Medicine, The First Affiliated Hospital of Nanjing Medical University, Jiangsu Province Hospital, Nanjing 210029, China

<sup>11</sup> Department of Infection, The First Affiliated Hospital of Nanjing Medical University, Jiangsu Province Hospital, Nanjing 210029, China

<sup>12</sup> Department of Anesthesiology and Pain Management, The First Affiliated Hospital of Nanjing Medical University, Jiangsu Province Hospital, Nanjing 210029, China

<sup>13</sup> Department of Nephrology, The First People's Hospital of Lianyungang, Lianyungang 222061, China

<sup>14</sup> Department of Nephrology, Northern Jiangsu People's Hospital, Yangzhou 225001, China

<sup>15</sup> Department of General Medicine, Geriatric Hospital of Nanjing Medical University, Nanjing 210024, China

<sup>16</sup> Department of Nephrology, BenQ Medical Center, The Affiliated BenQ Hospital of Nanjing Medical University, Nanjing 210019, China

<sup>17</sup> Department of Forensic Medicine, School of Basic Medical Sciences, Nanjing Medical University, Nanjing 211166, China

<sup>18</sup> Department of Human Anatomy, School of Basic Medical Sciences, Nanjing Medical University, Nanjing 211166, China

<sup>19</sup> Department of Outpatient Treatment Clinic, The First Affiliated Hospital of Nanjing Medical University, Jiangsu Province Hospital, Nanjing 210029, China

<sup>20</sup> Department of International Cooperation, The First Affiliated Hospital of Nanjing Medical University, Jiangsu Province Hospital, Nanjing 210029, China

<sup>21</sup> Department of Biological Specimen Repository, The First Affiliated Hospital of Nanjing Medical University, Jiangsu Province Hospital, Nanjing 210029, China

<sup>22</sup> Academy of Clinical and Translational Research, The First Affiliated Hospital of Nanjing Medical University, Jiangsu Province Hospital, Nanjing 210029, China

<sup>†</sup> These authors contributed equally to this work.

\* Correspondence to: Ningning Wang, E-mail: [wangnn@njmu.edu.cn](mailto:wangnn@njmu.edu.cn); Lianju Qin, E-mail: [ljqin@njmu.edu.cn](mailto:ljqin@njmu.edu.cn); Jiayin Liu, E-mail: [jyliu\\_nj@126.com](mailto:jyliu_nj@126.com)

Edited by Wei-Ping Jia

**Calciphylaxis is a rare disease characterized histologically by microvessel calcification and microthrombosis, with high mortality and no proven therapy. Here, we reported a severe uremic calciphylaxis patient with progressive skin ischemia, large areas of**

Received July 8, 2021. Revised November 23, 2021. Accepted February 7, 2022.

© The Author(s) (2022). Published by Oxford University Press on behalf of *Journal of Molecular Cell Biology*, CEMCS, CAS.

This is an Open Access article distributed under the terms of the Creative Commons Attribution-NonCommercial License (<https://creativecommons.org/licenses/by-nc/4.0/>), which permits non-commercial re-use, distribution, and reproduction in any medium, provided the original work is properly cited. For commercial re-use, please contact [journals.permissions@oup.com](mailto:journals.permissions@oup.com)

**painful malodorous ulcers, and mummified legs. Because of the worsening symptoms and signs refractory to conventional therapies, treatment with human amnion-derived mesenchymal stem cells (hAMSCs) was approved. Preclinical release inspections of hAMSCs, efficacy, and safety assessment, including cytokine secretory ability, immunocompetence, tumorigenicity, and genetics analysis *in vitro*, were introduced. We further performed acute and long-term hAMSC toxicity evaluations in C57BL/6 mice and rats, abnormal immune response tests in C57BL/6 mice, and tumorigenicity tests in neonatal Balbc-nu nude mice. After the preclinical research, the patient was treated with hAMSCs by intravenous and local intramuscular injection and external supernatant application to the ulcers. When followed up to 15 months, the blood-based markers of bone and mineral metabolism improved, with skin soft tissue regeneration and a more favorable profile of peripheral blood mononuclear cells. Skin biopsy after 1-month treatment showed vascular regeneration with mature noncalcified vessels within the dermis, and 20 months later, the re-epithelialization restored the integrity of the damaged site. No infusion or local treatment-related adverse events occurred. Thus, this novel long-term intravenous combined with local treatment with hAMSCs warrants further investigation as a potential regenerative treatment for uremic calciphylaxis due to effects of inhibiting vascular calcification, stimulating angiogenesis and myogenesis, anti-inflammatory and immune modulation, multidifferentiation, re-epithelialization, and restoration of integrity.**

**Keywords:** calciphylaxis, chronic kidney disease, vascular calcification, multidisciplinary rescue, human amnion-derived mesenchymal stem cells, preclinical research, regenerative medicine

## Introduction

Calciphylaxis is a rare, devastating disorder causing excruciatingly painful ischemic skin lesions due to microvascular calcification, microthrombosis, and endothelial injury, which results in infarction of tissues (Nigwekar et al., 2018). The annual incidence among patients with end-stage kidney disease reaches 0.04% (Brandenburg et al., 2017), and sepsis due to the infection of ulcerated wounds is a common cause of death (Seethapathy and Nigwekar, 2019). There is currently no approved therapy related to its rare incidence and poorly understood pathogenesis. In calciphylaxis patients receiving dialysis, 1-year mortality may reach 80% (McCarthy et al., 2016).

Stem cells are reported to be involved in angiogenesis, myogenesis, proliferation, and re-epithelialization of wound healing and play an important role in immune modulation, tissue remodeling, and extracellular matrix deposition (Hassanshahi et al., 2019). Human amnion-derived mesenchymal stem cells (hAMSCs) are abundant and compatible for use in allogeneic transplants, present a more 'youthful' phenotype, and have greater cell yields at harvest and enhanced immunomodulatory properties compared with human adipose-derived stem cells (hADSCs) and human bone marrow-derived stem cells (hBMSCs) (Topoluk et al., 2017). Importantly, hAMSCs have enhanced wound-healing properties through differentiation and stimulation of neoangiogenesis (Ertl et al., 2018).

Here, we reported a female uremic calciphylaxis patient in her 30s with large areas of painful malodorous ulcers and legs with a mummified appearance. This patient had been on peritoneal dialysis (PD) for 5 years and was admitted to The First Affiliated Hospital of Nanjing Medical University, Jiangsu Province Hospital, with multiple skin lesions accompanied by pain for >1 month. The patient had been switched to hemodialysis because of peritonitis and had progressive skin lesions with induration, plaques, purpura, livedo reticularis, and ecchymosis

on her back, thighs, lower limbs, and buttocks. The multiple, bilateral painful malodorous necrotic ulcerations were surrounded by leather-like skin.

The multiple medical problems included chronic kidney disease (CKD) G5D, which is defined as estimated glomerular filtration rate <15 ml/min/1.73 m<sup>2</sup> or requiring dialysis, calciphylaxis, skin and soft tissue infections, malnutrition, secondary hyperparathyroidism, PD-related tunnel infection, and hypertension. Treatments included nutritional support, antibiotic administration and infection control, low-calcium hemodialysis and continuous kidney replacement therapy, management of anemia and CKD–mineral and bone disorder (CKD–MBD), intravenous injection of sodium thiosulfate, wound care, pain management, anticoagulation, thrombosis prevention, cardioprotective and gastrointestinal protective therapy, and therapy for neurotrophic issues (Seethapathy and Nigwekar, 2019).

Because of the rapid progression of calciphylaxis refractory to conventional therapies, the patient began to receive hAMSC treatment as approved by the Ethics Committee of The First Affiliated Hospital of Nanjing Medical University, Jiangsu Province Hospital. Complete remission of calciphylaxis of the patient suggested that hAMSC therapy deserves further exploration as a regenerative treatment. To the best of our knowledge, this is the first report of the long-term intravenous combined with local treatment with hAMSCs, which is innovative for the uremic calciphylaxis patient.

## Results

### *Preclinical research of hAMSCs*

Quality control and preclinical research indexes of hAMSCs are listed in Table 1. The preparation and quality control of hAMSCs are described in detail in Materials and methods (Figure 7).

**Table 1** Quality control and preclinical research of cell line HAMSC10.

Measurement indicators	Testing items	Quality standards	Results
(1) Cell identity			
Cell morphology (QCP3–QCP6)	Cell shape	Fusiform	Up to standard
Genetic characteristics (QCP5)	Chromosome karyotype	46, XY/46, XX	46, XY
	STR map	Single origin	Up to standard
Cell surface antigens (QCP3–QCP6)	CD73, CD90, CD105, CD44	Positive cells $\geq$ 95%	Up to standard
	CD45, CD34, CD11b, CD19, HLA-DR	Positive cells $\leq$ 2%	Up to standard
(2) General biosafety			
Common microorganism contamination (QCP2–QCP6)	Fungus, bacteria, mycoplasma, <i>Treponema pallidum</i>	Negative	Up to standard
	Endotoxin	<0.5 EU/ml	Up to standard
(3) Endogenous and exogenous pathogenic factors			
Detection of virus infection by molecular analysis (QCP3 and QCP5)	HIV-1, HBV, HCV, EBV, HCMV, HHV6/7, HPV, retrovirus	Negative	Up to standard
Detection of virus infection by cell culture (QCP5)	Stem cell culture test	Normal morphology	Up to standard
	Hemadsorption/hemagglutination test	Negative	Up to standard
Detection of virus infection by animal inoculation (QCP5)	Guinea pig inoculation test <sup>a</sup>	Negative	Up to standard
(4) Cell viability and growth characteristics			
Cell viability (QCP2–QCP6)	Living cell counting	$\geq$ 95%	Up to standard
Growth curve analysis (QCP6)	Cell population doubling time	Report result	32.8 h
Cell cycle analysis (QCP5)	Cells in S-stage	Report result	12.8%
(5) Tumorigenicity			
<i>In vitro</i> tumorigenicity (QCP5)	Colon formation test, animal hypodermic inoculation test	Negative	Up to standard
<i>In vivo</i> tumorigenicity (QCP5)	Subcutaneous test in nude mice	Negative	Up to standard
(6) Biological potency			
Pluripotency (QCP5)	Adipogenic differentiation, osteogenic differentiation, chondrogenic differentiation	Positive	Up to standard
Cytokine secretory function (QCP5)	HGF	Report result	> 1000 pg/ml
	BDNF	Report result	> 100 pg/ml
	Nerve growth factor	Report result	> 10 pg/ml
Immunological effect (QCP5, AMSCs:PBMCs = 1:10)	Lymphocyte proliferation inhibition test	Report result	Lymphocyte proliferation inhibited
	Special lymphocyte subpopulation proliferation test (Th1/Th17/Treg)	Report result	Treg increased, Th1 and Th17 decreased

<sup>a</sup>Test methods were according to the *Pharmacopoeia of People's Republic of China* (2015 version, part III) except for that specially described in the Materials and methods section.

QCP, quality control point; STR, short tandem repeat; HIV-1, human immunodeficiency virus-1; HBV, hepatitis B virus; HCV, hepatitis C virus; EBV, Epstein-Barr virus; HCMV, human cytomegalovirus; HHV6/7, human herpes virus 6/7; HPV, human papillomavirus; PBMCs, peripheral blood mononuclear cells.

### Preclinical release inspections of hAMSCs

Release inspections consisted of general biosafety, viability, and growth characteristics were up to standard (Figure 1A). Cells positive for the surface antigens, including CD44, CD73, CD90, and CD105, were  $\geq$ 95%, while cells positive for CD11b, CD19, CD34, CD45, and human leucocyte antigen class II (HLA-II) were  $\leq$ 2%, which were up to quality standard (Figure 1B).

### hAMSC effective potency of cytokine secretory and immunocompetence function

hAMSC supernatants contained high levels of hepatocyte growth factor (HGF,  $7166.2 \pm 1425.6$  pg/ml), angiogenic factors including angiopoietin-1 (Ang-1,  $10337.5 \pm 172.3$  pg/ml), brain-derived neurotrophic factor (BDNF,  $1658.8 \pm 144.9$  pg/ml), and interleukin-6 (IL-6,  $9655.5 \pm 1588.3$  pg/ml) and moderate levels of vascular endothelial growth factor (VEGF,  $167.6 \pm 89.2$  pg/ml), fibroblast growth factor-7 (FGF-7,  $654.7 \pm 188.2$  pg/ml), and

interleukin-12 (IL-12,  $256.4 \pm 158.7$  pg/ml) (Figure 1C). The hAMSCs had regulatory functions in immune cells, especially T cells, which could slightly inhibit the proliferation rate of total lymphocytes ( $-5.2\% \pm 0.4\%$ ), strongly inhibit the proliferation rate of T helper 1 (Th1) ( $-45.5\% \pm 2.0\%$ ), Th2 ( $-39.8\% \pm 8.1\%$ ), and Th17 ( $-32.6\% \pm 22.7\%$ ) cells, and promote the proliferation rate of regulatory T (Treg) cells ( $20.0\% \pm 6.3\%$ ) (Figure 1D).

### hAMSC safety assessment on tumorigenicity in vitro and in vivo

A soft agar colony formation experiment was performed. After 3 weeks, no colony was observed in the negative control group of human normal embryo lung fibroblasts (MRC-5, Figure 2A) and the hAMSC group (Figure 2B). In contrast, the positive control group of human cervical cancer cells (Hela) had evident colony formation, with the colony number of  $232.7 \pm 20.4$  and the colony formation rate of  $7.76\% \pm 0.68\%$  (Figure 2C). Furthermore, subcutaneous tests in nude mice (Balbc-nu) were performed. During the observation period for 16 weeks, there was no tumor formation in the negative control group (HEF5.2

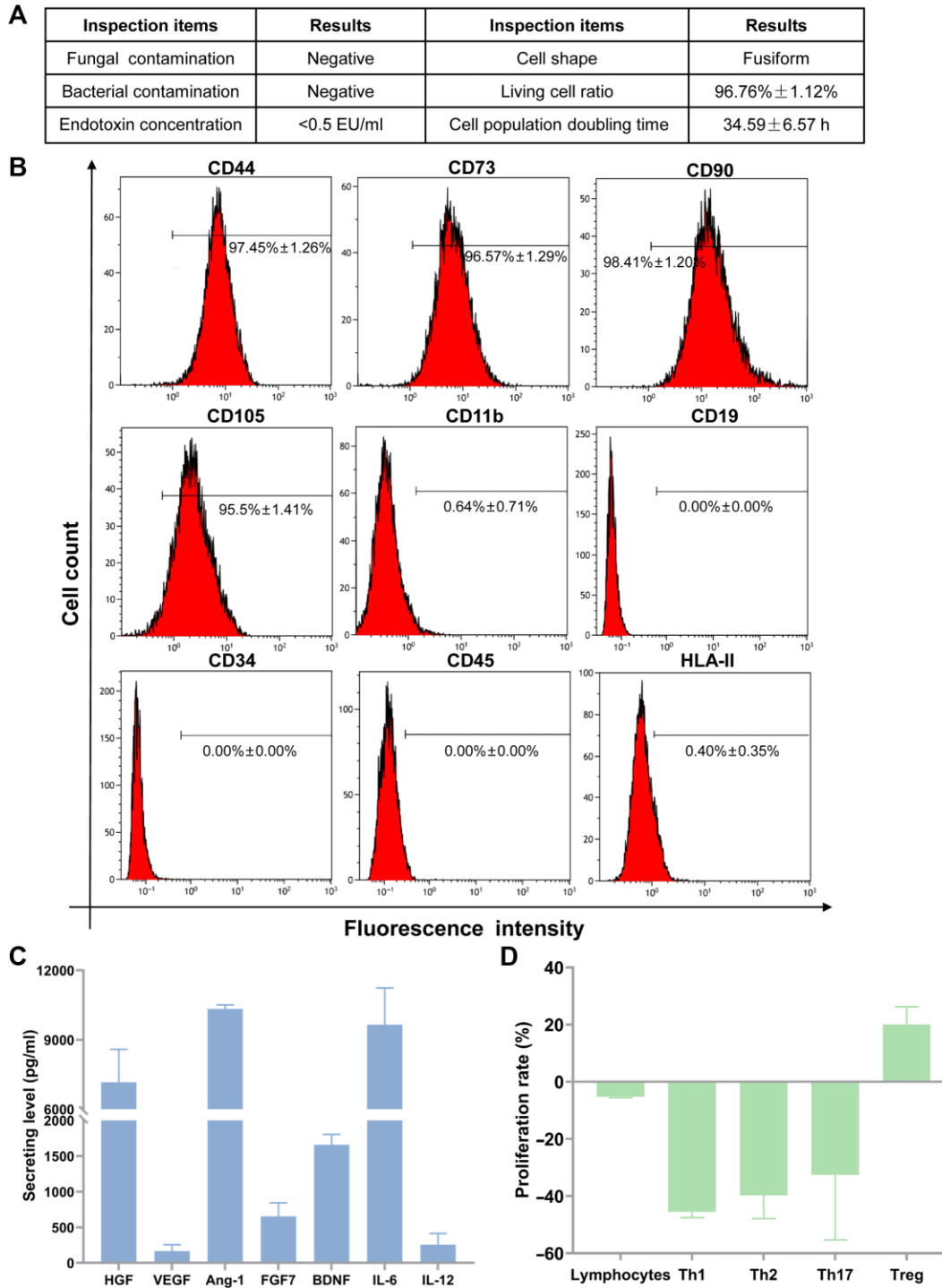


**Figure 1** Preclinical release inspections and efficacy assessment. **(A)** General biosafety and cell viability of hAMSCs were up to quality standard. **(B)** Release inspections on hAMSC surface antigens. **(C)** Analysis for cytokine secretions from hAMSC culture supernatants. **(D)** hAMSCs showed immunocompetence *in vitro* when cocultured with lymphocytes from healthy persons.

cells, **Figure 2D**) and the hAMSC group (**Figure 2E**), while large tumors were observed in the positive control group (NCI-H460, **Figure 2F–H**). Our data demonstrated that the tumorigenic potential of hAMSCs was negligible both *in vitro* and *in vivo*.

#### *hAMSC safety assessment on genetics*

G-banding analysis showed that the karyotype was normal (46, XY) and STR analysis suggested that the cells were a single source population (Supplementary Figure S1).

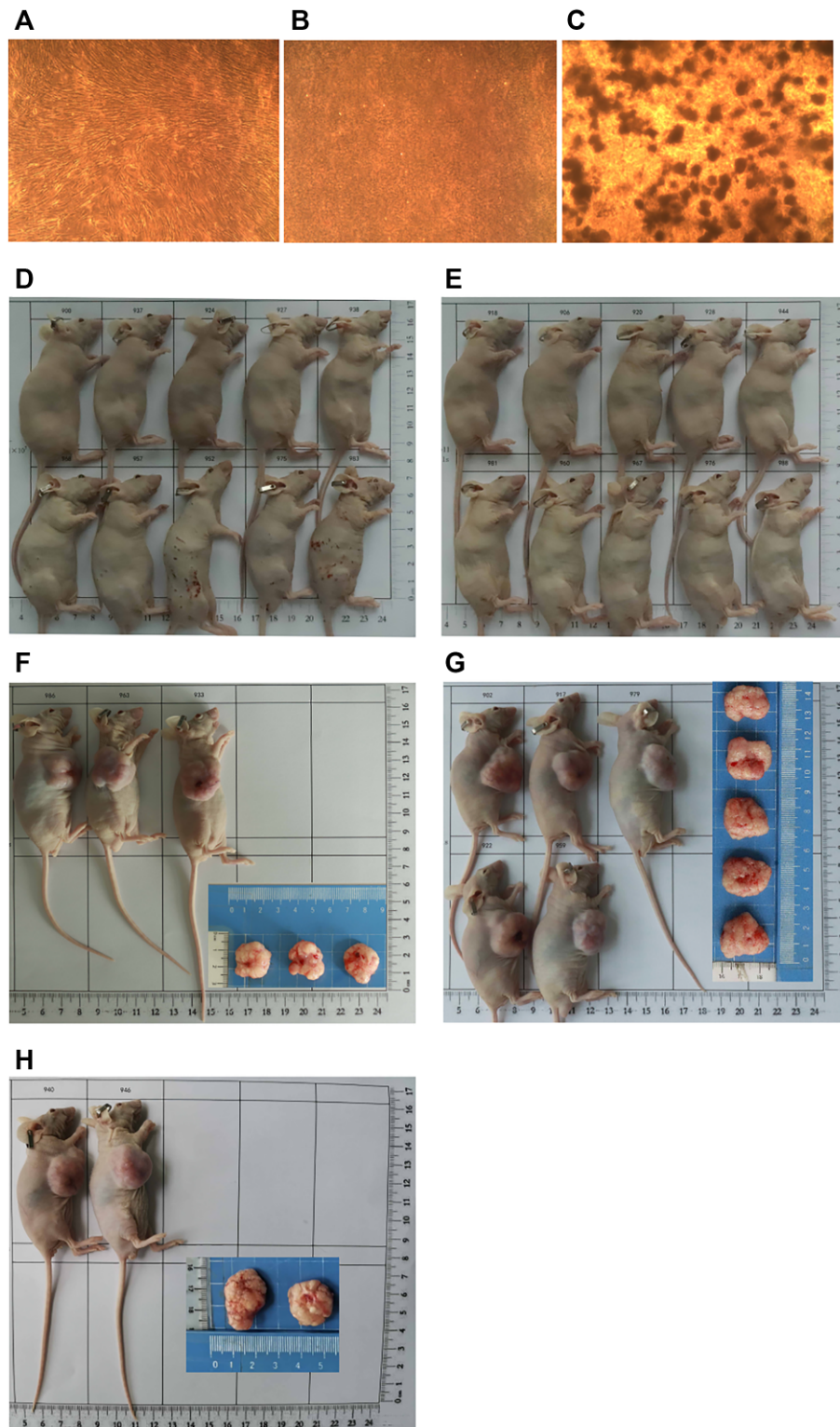


**Figure 2** Preclinical hAMSC tumorigenicity assessments *in vitro* and *in vivo*. (A–C) The soft agar colony experiment was performed to investigate the tumorigenicity of hAMSCs cultured for 21 days *in vitro* (magnification, 40×). (A) Human normal embryo lung fibroblasts (MRC-5,  $3.0 \times 10^3$  cells/well) were negative controls. (B) hAMSCs ( $6.0 \times 10^3$  cells/well) showed no tumorigenic effect. (C) Human cervical cancer cells (HeLa,  $3.0 \times 10^3$  cells/well) were used as positive controls. (D–H) Subcutaneous tests in nude mice (Balbc-nu) were performed to investigate the tumorigenicity of hAMSCs *in vivo*. The negative control group (D) and hAMSC group (E) did not show tumor formation after 16 weeks. In the positive control group (NCI-H460), the mice were sacrificed when tumor arose and grew to 3000 mm<sup>3</sup> at Day 26 (F), Day 30 (G), and Day 33 (H), respectively.

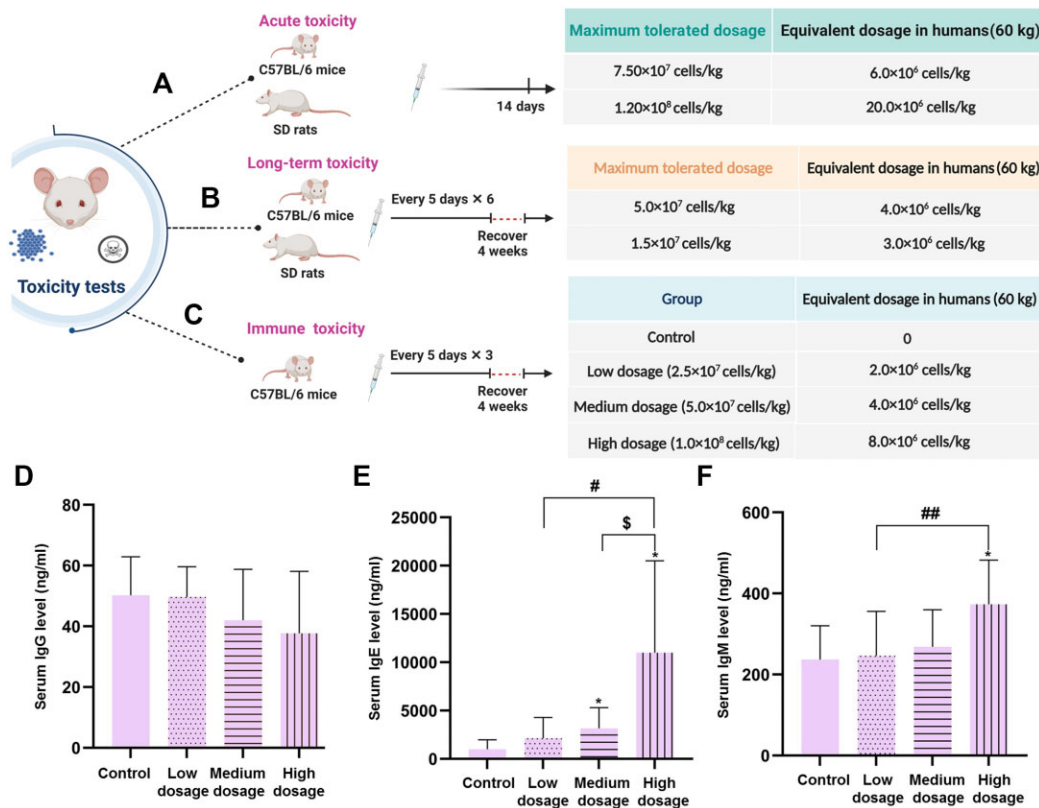


**Figure 3** Animal tests for maximum tolerated dosages and immune toxicity of hAMSCs. (A and B) Maximum tolerated hAMSC dosages in C57BL/6 mice and SD rats were investigated with acute (A) and long-term (B) toxicity tests. (C) Immune toxicity of hAMSCs in C57BL/6 mice was investigated in control, low-dosage, medium-dosage, and high-dosage groups. The estimated equivalent dosages in humans are listed. Created with BioRender.com. (D–F) Serum IgG (D), IgE (E), and IgM (F) levels were detected in immune toxicity tests. \* $P < 0.05$  vs. control group;  $^{\$}P < 0.05$  vs. medium-dosage group;  $^{\#}P < 0.05$  and  $^{\#\#}P < 0.01$  vs. low-dosage group.

*Maximum tolerated dosages in mice/rats and the estimated equivalent dosages in humans*

The dosage conversion between mice/rats and humans was not only based on the body mass as functional biochemical systems vary among different species (Nair and Jacob, 2016). For a man whose body weight is 60 kg and body surface area is  $1.53 \text{ m}^2$ , the intravenous administration dosage of hAMSCs is  $1.0 \times 10^6$  cells/kg. Here, we used the Mech formula to determine surface area, a classical approach to estimate equivalent dosages between humans and mice/rats (Nair et al., 2018). The formula is expressed as  $S = KW^{2/3}$ , in which  $S$  is the surface area in square centimeters,  $W$  is the weight in kilograms, and  $K$  is a constant (Meeh, 1879).

The maximum tolerated dosage in C57BL/6 mice was  $7.50 \times 10^7$  cells/kg (~6 times for the clinical intravenous administration dosage, equivalent to  $6.0 \times 10^6$  cells/kg in humans). The maximum tolerated dosage in Sprague–Dawley (SD) rats was  $1.20 \times 10^8$  cells/kg (~20 times for the clinical intravenous administration dosage, equivalent to  $20.0 \times 10^6$  cells/kg in humans) (Figure 3A).

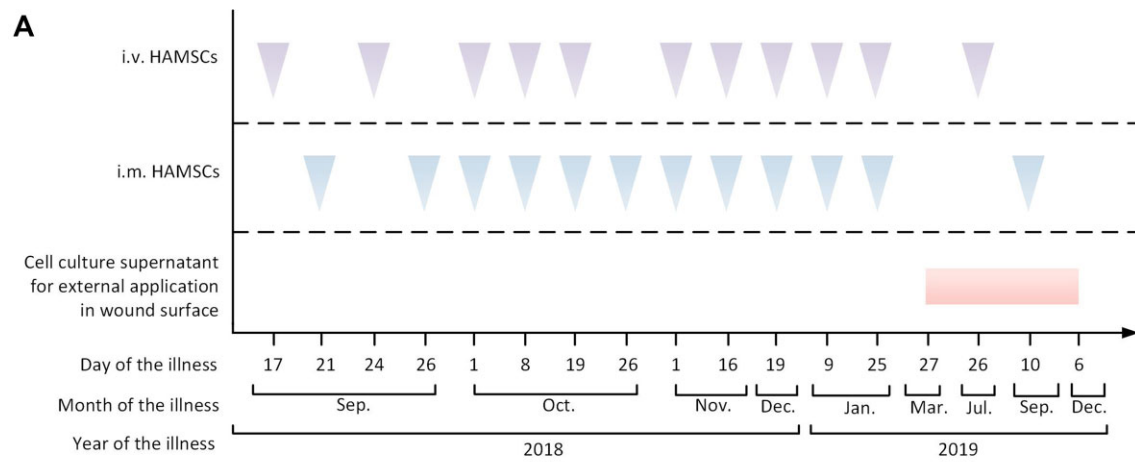
High-dosage hAMSCs can cause pulmonary vascular embolism and death in mice. There was no significant toxicity in

C57BL/6 mice within a hAMSC dosage of  $5.0 \times 10^7$  cells/kg (equivalent to  $4.0 \times 10^6$  cells/kg in humans). No significant toxicity was observed in SD rats within a hAMSC dosage of  $1.5 \times 10^7$  cells/kg (equivalent to  $3.0 \times 10^6$  cells/kg in humans) (Figure 3B). These C57BL/6 mice and SD rats were normal in body weight, organ coefficients, histopathological analysis, bone marrow smear, blood routine and biochemical tests, and blood interferon-gamma (IFN- $\gamma$ ) levels (data not shown).

*Immune toxicity tests in mice with hAMSC intravenous administration*

Three dosages of hAMSCs were injected intravenously to assess immune toxicity in C57BL/6 mice (Figure 3C). After the first hAMSC intravenous administration, one male mouse in the high-dosage group ( $1.0 \times 10^8$  cells/kg) died because of pulmonary embolism. The appearance and behavior of surviving mice in each group were normal.

Among the control, low-dosage, medium-dosage, and high-dosage hAMSC groups, serum immunoglobulin G (IgG) levels were not significantly different (Figure 3D). Serum immunoglobulin E (IgE) levels increased in a dosage-dependent manner, especially in the medium-dosage and high-dosage groups



The patient was not hospitalized from January 28, 2019 to March 12, 2019.

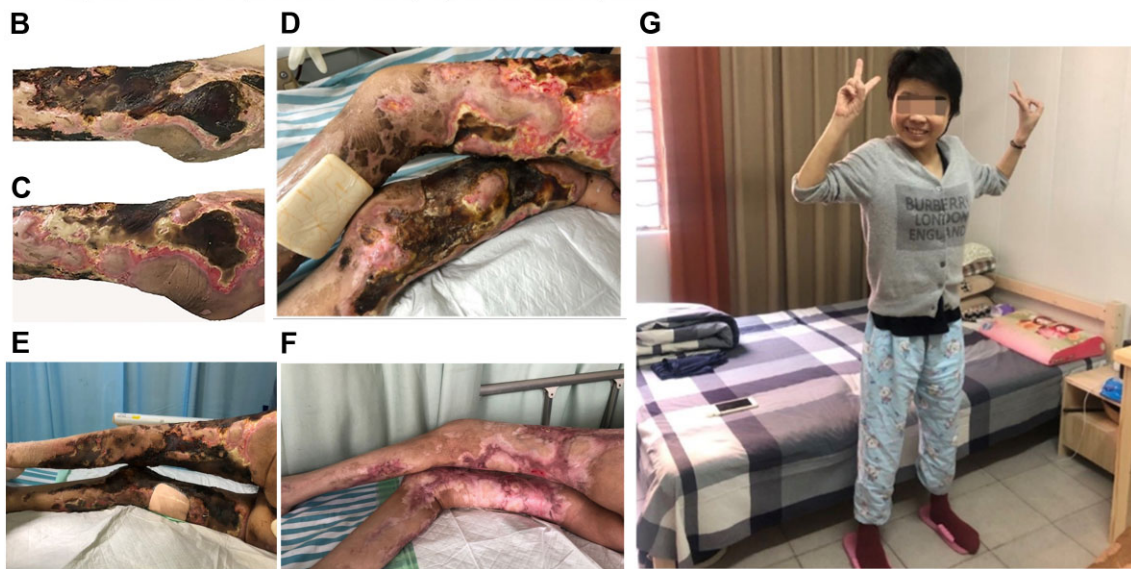


**Figure 4** Clinical hAMSC treatment for the uremic calciphylaxis patient. **(A)** An overview of the hAMSC therapeutic schedule for the patient. **(B)** Wounds on the lower limbs before hAMSC treatment. **(C)** After 14 days of intravenous infusion plus local intramuscular injection, the surface of wounds began to recover. **(D)** The left thigh with local intramuscular hAMSC injection for 1 month recovered better than the right thigh without local intramuscular injection. **(E)** Wounds of lower limbs before treatment. **(F)** Skin lesions were healed after treated with hAMSCs for 1 year. **(G)** The patient could walk after 15 months of hAMSC treatment.

(Figure 3E). Serum immunoglobulin M (IgM) levels showed a dosage-dependent increasing trend after hAMSC intravenous administration, especially in the high-dosage group (Figure 3F). Our results demonstrated that there was no significant immune toxicity in C57BL/6 mice within the dosage of  $5.0 \times 10^7$  cells/kg (equivalent to  $4.0 \times 10^6$  cells/kg in humans).

#### Treatment course and dosages of hAMSCs for the uremic calciphylaxis patient

Prior to clinical hAMSC treatment, the patient's hAMSC-lysate skin test showed negative. Then, hAMSCs were administered intravenously to the patient at a dosage of  $1.0 \times 10^6$  cells/kg body weight, combined with local intramuscular injection along

the wound edge ( $2.0 \times 10^4$  cells/cm<sup>2</sup>) and external application of the cell culture supernatants on wound surface. The patient's hAMSC treatment course is outlined in Figure 4A.

#### Healing progress of skin lesions treated with hAMSCs

Before treatment, the wounds showed multi-necrotizing ulcers with eschar and infection (Figure 4B). After intravenous plus local intramuscular hAMSC injection for 14 days, the skin lesions had substantially improved (Figure 4C). During the early stage of calciphylaxis, the patient was in great pain, not fully relieved by analgesics, and had evident difficulty when it was necessary to change body position. Hence, we first gave intramuscular hAMSC injection in the left thigh alone. After 1 month, when reduced eschar and regenerative tissue were observed, it was

clear that the left thigh was healed better than the right one (Figure 4D), indicating that local injection could accelerate the wound recovery. Compared with pre-therapy (Figure 4E), the lower limbs were successfully cured after 1 year (Figure 4F), and the general condition of the patient was visually improved after 15 months (Figure 4G).

#### Adverse events

No infusion or local treatment-related adverse events occurred.

#### Measurements of blood parameters

After hAMSC treatment, hemoglobin and serum albumin levels gradually increased. The levels of leukocytes, platelets, and high-sensitivity C-reactive protein decreased substantially, suggesting improvement of inflammation status. A moderate rebound in serum phosphorus and alkaline phosphatase levels was observed because of poor control on the diet. However, serum calcium and intact parathyroid hormone (iPTH) levels remained in the normal range of the treatment target (Figure 5A–I). Furthermore, serum tumor markers were stable in normal range after hAMSC treatment for 15 months (Figure 5J–M).

#### Subpopulations of PBMCs after hAMSC treatment

The patient had elevated Th1/Th2/Th17 baseline levels, a higher Th1/Th2 ratio (6.25:1), and a lower Treg level. After the first month of hAMSC treatment, Th1 and Treg cells increased (22.71% and 303.06%, respectively), while Th2 and Th17 cells decreased (−45.76% and −32.52%, respectively). After 15 months of hAMSC treatment, Th1/Th2/Th17 cells were repressed (−52.41%, −33.47%, and −99.19%, respectively) and the proliferation of Treg cells was enhanced (93.33%). Importantly, the patient had an improved Th1/Th2 ratio (4.47:1), which was closer to the normal value (2:1), after 15 months of hAMSC treatment (Figure 5N–Q).

#### Hematoxylin and eosin staining of skin biopsy from the calciphylaxis patient during the course of hAMSC treatment

Hematoxylin and eosin (H&E) staining of skin biopsy obtained from the margin of an ulcer on the thigh before hAMSC treatment revealed exfoliation of the epidermis, necrosis, inflammation, and vascular calcification (Figure 6A–D). After 1 month of hAMSC treatment, skin biopsy from the thigh displayed nascent granulation tissue, regeneration of noncalcified blood vessels, reduced inflammatory response, and no epidermal tissue (Figure 6E–G). After 20 months of hAMSC treatment, skin histological characteristics displayed regeneration of epidermal and dermal layers, mature vessels without calcification, collagen remodeling, and mild inflammation. This process, termed re-epithelialization, restored the integrity of the damaged site (Figure 6H–I).

Skin biopsy statistical analysis of inflammatory cells and blood vessels during hAMSC treatment by light microscopy is shown in Supplementary Table S1.

## Discussion

In this study, the uremic patient was diagnosed with calciphylaxis based on typical clinical manifestations such as severely painful skin lesions and skin histopathological findings. This patient was refractory to a session of medical management strategies, including intravenous administration of sodium thiosulfate (Peng et al., 2018), wound care, pain management, anticoagulation, thrombosis prevention, co-interventions of lower dialysate calcium concentration and increased length or frequency of dialysis sessions, etc. (Nigwekar et al., 2018).

Arteriolar calcification due to vascular smooth muscle cell (VSMC) phenotype transdifferentiation plays a crucial role in the pathogenesis of calciphylaxis (Nigwekar et al., 2018). Intravenous ADSC treatment has been reported to suppress thoracic arterial medial calcification in CKD rats (Yokote et al., 2017). BMSC-derived exosomes could inhibit high phosphate-induced aortic calcification by decreasing the high mobility group box 1 (HMGB1) level via the sirtuin 6–HMGB1 deacetylation pathway (Wei et al., 2021). BMSC-derived exosomes inhibited high phosphorus-induced VSMC calcification *in vitro* by modifying miRNA profiles involved in the Wnt, mammalian target of rapamycin, or mitogen-activated protein kinase signaling pathway (Guo et al., 2019) and regulating the nuclear factor kappa-B (NF- $\kappa$ B) axis (Liu et al., 2021a).

In addition to treatment of vascular calcification, stem cells can promote neovascularization by multi-differentiation into keratinocytes, endothelial cells, or VSMCs and act as perivascular cells. Paracrine secretions of cytokines, growth factors, microvesicles/exosomes, and chemokines can modulate angiogenesis, apoptosis, and immune responses and facilitate the regeneration of damaged tissue (Zhao et al., 2017; Hassanshahi et al., 2019).

Our research indicated that hAMSC supernatants contained high levels of cytokines. As an upstream-indirect proangiogenic growth factor, HGF stimulates endothelial cells to proliferate and migrate while inhibiting cell apoptosis and tissue reconstruction (Pang et al., 2018), inducing VEGF and blood vessel formation (Jiao et al., 2016a). HGF is also a potent immunomodulatory and anti-inflammatory factor (Maraldi et al., 2015; Pang et al., 2018). Ang-1 is reported to accumulate in the extracellular matrix, enhancing the recruitment of pericytes and SMCs, promoting endothelial cell survival, proliferation, migration, and angiogenesis (Wang et al., 2019).

BDNF stimulates new vessel formation by increasing VEGF, regulates the primary proinflammatory transcription factors such as NF- $\kappa$ B, and restricts the magnitude of the inflammatory response (Halade et al., 2013). Muscle-derived BDNF plays a role in muscle repair, regeneration, and differentiation (Pedersen, 2013). IL-6 has mitogenic and proliferative effects on keratinocytes and is chemoattractive to neutrophils (Barrientos et al., 2008; Cañedo-Dorantes and Cañedo-Ayala, 2019). As a pro-angiogenic factor, IL-6 can regulate endothelial progenitor cell migration (Fan et al., 2008), activate quiescent microvascular endothelial cells, and induce the formation of tubular

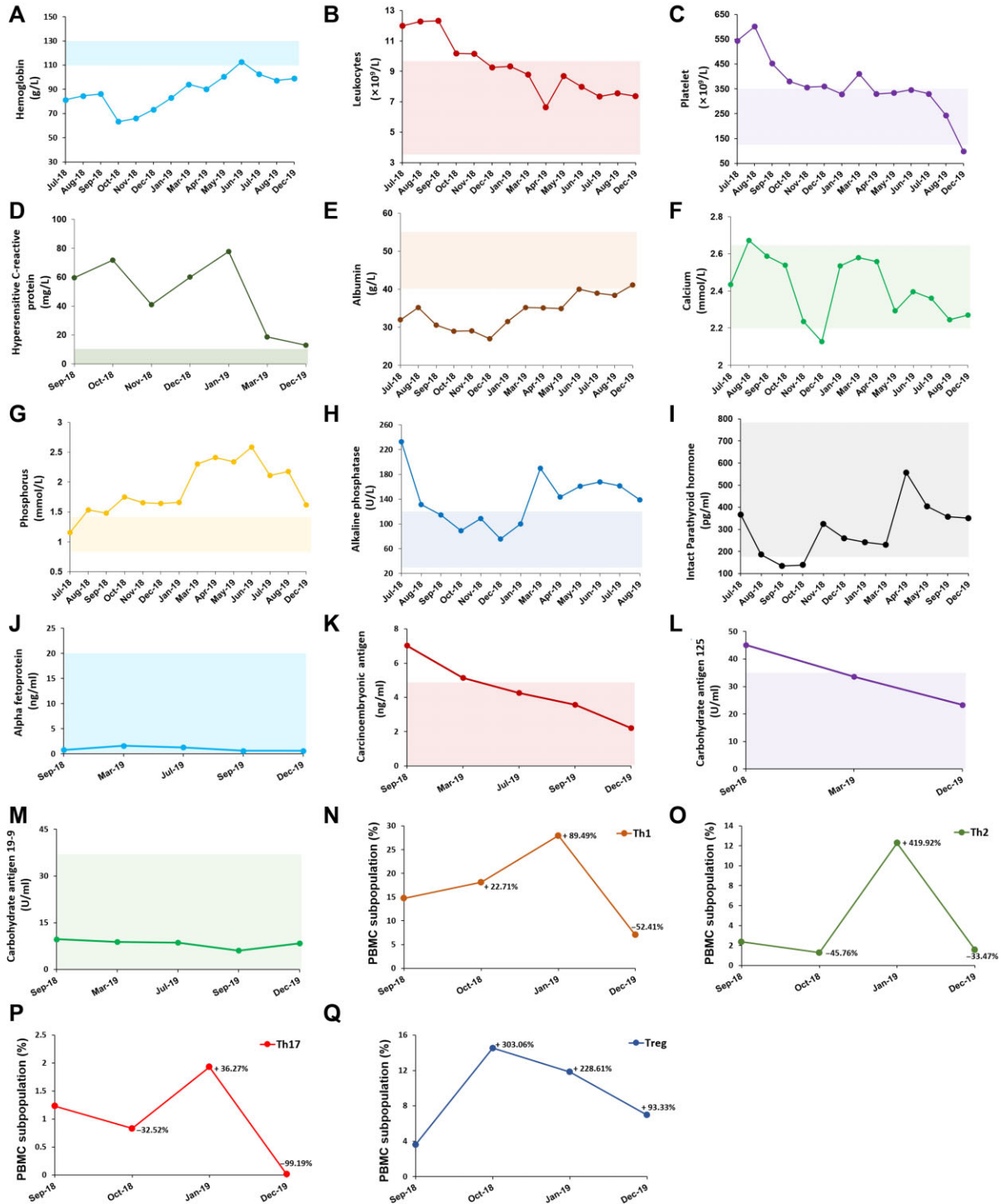


**Figure 5** The laboratory data of the uremic calciphylaxis patient before and after hMSC treatment. (A–M) After applying hMSC treatment, the levels of hemoglobin (A), leukocytes (B), platelet (C), hypersensitive C-reactive protein (D), serum albumin (E), serum calcium (F), serum phosphorus (G), serum alkaline phosphatase (H), serum intact parathyroid hormone (I), serum alpha fetoprotein (J), serum carcinoembryonic antigen (K), serum carbohydrate antigen 125 (L), and serum carbohydrate antigen 19-9 (M) were monitored. Shaded area shows the reference range of each indicator. The hemoglobin, calcium, phosphorus, and intact parathyroid hormone levels are based on the recommended ranges (KDIGO Clinical Practice Guideline for Anemia in Chronic Kidney Disease, 2012; [Kidney Disease: Improving Global Outcomes \(KDIGO\) CKD–MBD Update Work Group, 2017](#)), and others are based on the normal reference values of laboratory tests. (N–Q) PBMC subpopulations of the patient during the course of hMSC treatment, including Th1 (N), Th2 (O), Th17 (P), and Treg (Q), were detected.

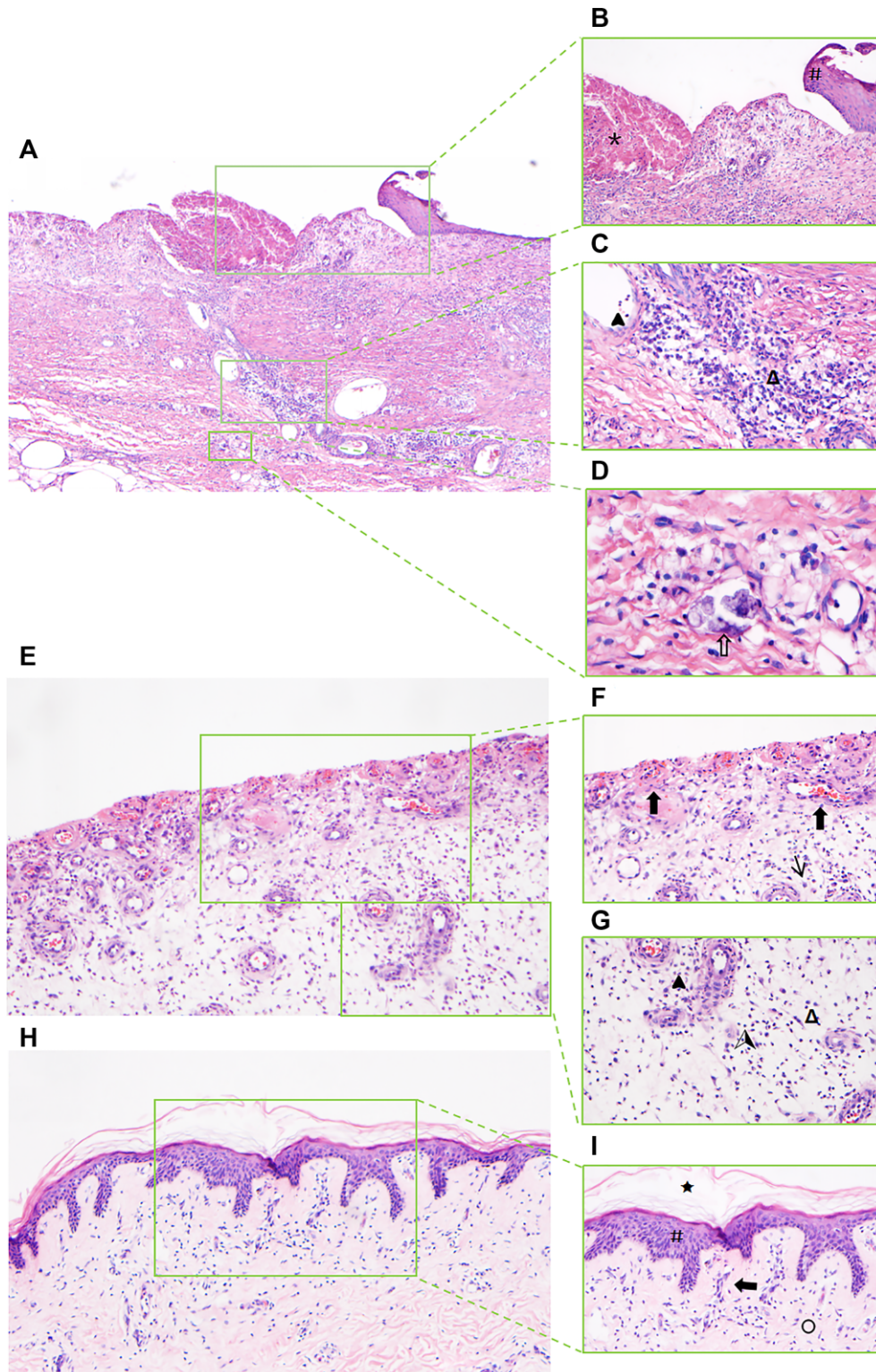


**Figure 6** H&E staining of skin biopsy from the calciphylaxis patient during hAMSC treatment. (A–D) Specimens of biopsy obtained from the margin of an ulcer on the thigh before hAMSC treatment. (A) Pathological characteristics contain exfoliation of epidermis, necrosis, inflammation, and vascular calcification (magnification, 40×). (B) Exfoliation of epidermis (#), necrosis (\*), and marked inflammatory response (magnification, 100×). (C) Extensive infiltration of inflammatory cells mainly presented as plasmacytes (Δ) and neutrophils (▲) (magnification, 200×). (D) Sheet-like calcium deposits on the wall of small vessels (↑) characterized as granular basophilic plaque (400×). (E–G) Skin biopsy from the thigh of the calciphylaxis patient after hAMSC treatment for 1 month.

structures (Potente et al., 2011; Wang et al., 2012). IL-6 is essential for maturation, proliferation, differentiation, and maintenance of B cells/plasma cells and proinflammatory Th17 and Th2 cells (Tvedt et al., 2017). Furthermore, IL-6 is linked with muscle stem cells and has myogenesis effects (Pedersen, 2013).

VEGF affects most downstream activities of angiogenesis, including endothelial cell proliferation, migration, invasion, and survival, and promotes vascular permeability (Waldner et al., 2010; Hu et al., 2019). VEGF also induces extravascular leakage of plasma proteins, modulates extracellular matrix proteolysis (Bien et al., 2015), regulates local immune response, and helps recover from inflammation (Cañedo-Dorantes and Cañedo-Ayala, 2019). FGF-7 can contribute to synthesizing various pro-angiogenic molecules, including VEGF, to promote angiogenesis (Qu et al., 2018). As a keratinocyte growth factor, FGF-7 is upregulated after skin injury, stimulates the proliferation (Kao et al., 2011) and migration (Qu et al., 2018) of keratinocytes, and accelerates wound healing by re-epithelialization (Iwamoto et al., 2015). FGF-7 is important for the formation of hair follicles (Qu et al., 2018). IL-12 induces Th0 to Th1 cells to enhance cellular immunity (Zhou et al., 2019), promotes the cytotoxic activity of natural killer (NK) and T lymphocytes, and increases the secretion of cytokines, including IFN- $\gamma$  and tumor necrosis factor- $\alpha$  (Zhao et al., 2020).

MSCs can regulate both innate immunity and adaptive immunity by modulating activation, maturation, proliferation, or cytolytic activity of multiple immune cells, including T, B, and NK lymphocytes, dendritic cells, monocytes, and macrophages (Shi et al., 2018). In this calciphylaxis patient, an increase in the Th1/Th2 ratio at baseline indicated that inflammation reactions were triggered and Th1/Th2 balance was broken (Chi et al., 2019). After 15 months of hAMSC treatment, a gradual decrease in the Th1/Th2 ratio revealed inflammation suppression and improved health. The anti-inflammatory properties of MSCs have been linked to their immunoregulation potential (Mishra et al., 2020). Consistent with previous studies (Shi et al., 2018; Harrell et al., 2020), our research suggested that hAMSCs could suppress the proliferation and differentiation of Th1/Th17 cells, induce functional Treg cells, and promote cell regeneration.

The use of hAMSCs in animal models of various diseases has been documented previously. Long-term effects of intravenous hAMSC administration for amyotrophic lateral sclerosis were investigated in superoxide dismutase (SOD1<sup>G93A</sup>) mice. After being treated with hAMSCs ( $1 \times 10^6$  cells) at the 12th, 14th, and 16th week, the mice displayed retarded disease progression and extended survival (Sun et al., 2014). hAMSCs ( $1 \times 10^6$  cells) administered intravenously can ameliorate spatial learning and memory function in C57BL/6J-amyloid precursor protein (APP)

transgenic mice with Alzheimer's disease after 3-week treatment (Jiao et al., 2016b).

hAMSCs are also reported to treat skin lesions with local injection. C57BL/6 mice with a deep second-degree burn on the skin were injected with hAMSCs subcutaneously ( $2 \times 10^6$ ) near the wound. hAMSCs and conditional medium could cure skin injury by inhibiting apoptosis and promoting proliferation (Li et al., 2019). In C57BL/6 mice with full-thickness skin wound, 100  $\mu$ l of cell suspension containing  $1 \times 10^7$  hAMSCs/ml in phosphate-buffered saline (PBS) was subcutaneously injected along the wound edge, which could contribute to the macrophages' transformation from M1 type to M2 type, inducing upregulation of anti-inflammatory and anti-fibrotic factors and downregulation of inflammation-mediated factors (Shi et al., 2020). In SD rats with full-thickness skin defect wounds, hAMSCs injected at the dosages of  $0.5 \times 10^4$ ,  $0.5 \times 10^5$ , and  $0.5 \times 10^6$  cells were reported to promote wound healing and epithelialization after 15 days (Gao et al., 2020). In SD rats defecting in the middle of tibialis anterior muscle, gelatin methacryloyl hydrogel with hAMSCs ( $5 \times 10^5$ /ml) was implanted into the defect area, which displayed agglomeration of cells after 2 weeks (Zhang et al., 2019).

Based on the above references about intravenous/local hAMSC injection and our animal experiments for maximum tolerated dosages, we designed an hAMSC therapeutic schedule for this uremic calciphylaxis patient with the approval of the Ethics Committee of The First Affiliated Hospital of Nanjing Medical University, Jiangsu Province Hospital. The patient was treated with hAMSCs by intravenous and local intramuscular injection within safe dosages. Furthermore, hAMSC supernatant was applied to her ulcers. The patient could tolerate well with skin regeneration. Skin biopsy from her thigh showed viable skin with revascularization without calcification after hAMSC treatment for 1 month and integrated skin tissue after hAMSC treatment for 20 months. However, the patient died due to cerebral hemorrhage in May 2020. We speculated that the death was not directly related to stem cell treatment because intravenous and intramuscular injections had been stopped for 8 months at her death.

In conclusion, hAMSC treatment for this patient appeared to promote skin and soft tissue repair, which we speculate may have resulted from the inhibition of vascular calcification, the stimulation of neovascularization and myogenesis, as well as enhanced anti-inflammatory activity, immunoregulatory actions, and re-epithelialization (Figure 8). This case provides evidence and rationale for using hAMSCs as a novel candidate for regenerative treatment in uremic calciphylaxis patients.

**Figure 6 (Continued)** (E) Pathological characteristics contain nascent granulation tissue, reduced inflammatory response, and no epidermal tissue (magnification, 100 $\times$ ). (F) Proliferation of myofibroblasts ( $\uparrow$ ) and regeneration of blood vessels ( $\uparrow$ ) (magnification, 200 $\times$ ). (G) Reduced plasmacytes ( $\Delta$ ), neutrophils ( $\blacktriangle$ ), and lymphocytes ( $\blacktriangle$ ) in the subcutaneous tissue (magnification, 200 $\times$ ). (H and I) Skin biopsy from the thigh of the calciphylaxis patient after hAMSC treatment for 20 months. (H) Pathological characteristics contain regeneration of epidermal and dermal layers, mature vessels without calcification, collagen remodeling, and mild inflammation (magnification, 100 $\times$ ). (I) Intact cuticle ( $\star$ ), restoration of damaged epidermis integrity ( $\#$ ), collagen fiber ( $\ominus$ ), and fewer inflammatory cells (magnification, 200 $\times$ ).

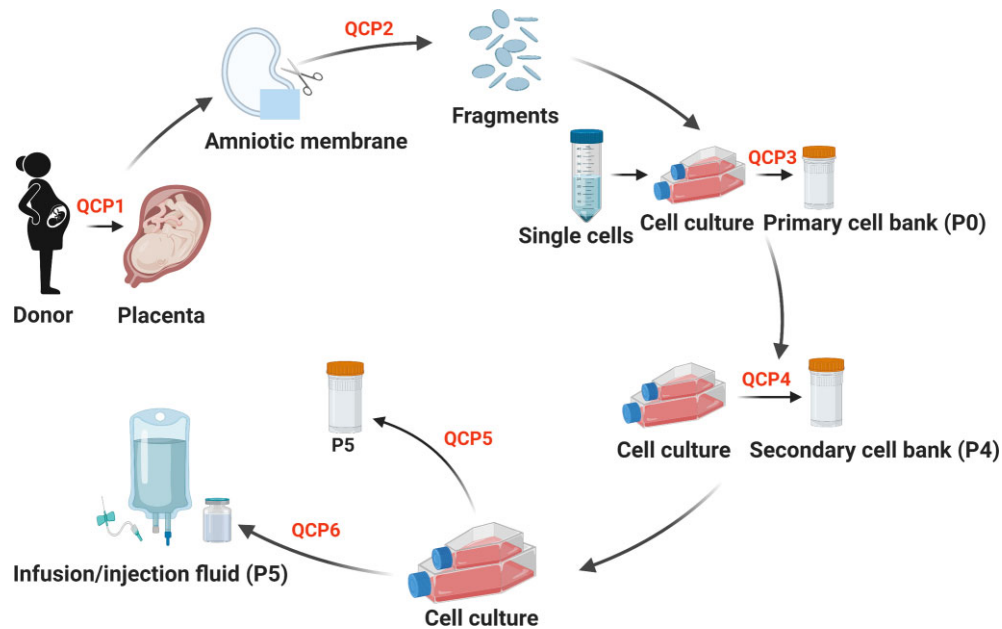


**Figure 7** The flowchart of manufacture and preclinical quality control for hAMSCs. At QCP1, virus infection by viruses such as HIV-1, HBV, HCV, EBV, HCMV, HHV6/7, HPV, and retrovirus was tested, medical history was inquired (excluding donors with contraindication), and fetus health and body weight were assessed. At QCP2, microbial contaminations (fungus, bacteria, mycoplasma, and *Treponema pallidum*) were tested. At QCP3 and QCP4, microbial contamination and levels of surface markers were analyzed. At QCP5, karyotype and STR were confirmed, microbial contamination, cell viability, and levels of surface markers were tested, and oncogenicity *in vitro*, cytokine secretory ability, and immunocompetence of hAMSCs were analyzed. At QCP6, microbial contamination, cell shape, cell viability, cell growth, and levels of surface markers were analyzed. Created with BioRender.com.

## Materials and methods

### Preparation and quality control of produced hAMSCs

hAMSCs were prepared in the State Key Laboratory of Reproductive Medicine, The First Affiliated Hospital of Nanjing Medical University, Jiangsu Province Hospital (Liu et al., 2021b), a Good Manufacturing Practice (GMP)-compliant laboratory according to the national principle ('Guiding Principle for Cell Therapy Products Research and Assessment Technique', 2017).

Human amniotic membranes were donated by healthy pregnant women (Figure 7, QCP1). Amniotic membranes screened negative for microbial contamination were cultured (Figure 7, QCP2). Primary hAMSCs (P0) were cryopreserved as primary cells in our cell bank if negative for microbial and virus contamination (Figure 7, QCP3). P0 cells were passaged three times and cryopreserved as the secondary cell bank after confirmed negative microbial contamination (Figure 7, QCP4). Safety and efficacy assessments (Figure 7, QCP5) included microbiology, virology, viability, cell surface antigen, morphology, tumorigenicity, secretory ability, and immunocompetence analysis, as well as genetics analysis of karyotype and STR ('Guiding Principle for Stem Cell-based Medicinal Products Quality Control and Pre-clinical Research', 2015; 'Guiding Principle for Cell Therapy Products Research and Assessment Technique', 2017). The hAMSCs passed the quality verification from the National Institutes for Food and Drug Control of China (reports of SH201905141 and SH201905142). The secondary cell bank produced fresh hAMSCs after going through the release

inspections (Figure 7, QCP6). Establishment and quality control of hAMSC lines are introduced in the following sections (Alviano et al., 2007; 'Guiding Principle for Stem Cell-based Medicinal Products Quality Control and Pre-clinical Research', 2015).

### Establishment of hAMSC lines

Human amniotic membranes were digested by CTS™ TrypLE™ Select Enzyme (Gibco) and Collagenase NB 6 GMP Grade (Serva GmbH). Digested cells were plated in 15-cm dishes and cultured in a 37°C, 5% CO<sub>2</sub> incubator for 4–5 days. The complete culture medium was composed of 5% UltraGRO-hPL (Helios Bioscience), MEM-alpha (Gibco), 1% L-glutamine (Gibco), and 2 U/ml heparin sodium. Cells that reached 80%–90% confluence were digested by CTS™ TrypLE™ Select Enzyme. The harvested cells were cryopreserved or passaged further to perform the quality test.

### Release inspections on hAMSCs

hAMSC-specific surface markers were detected by flow cytometry. Fungal and bacterial contamination was tested by culture methods according to the national principle ('Guiding Principle for Cell Therapy Products Research and Assessment Technique', 2017), and bacterial contamination was further assessed by an endotoxin detection kit (Zhanjiang Bokang Marine Biological Co., Ltd). Mycoplasma infection was assessed by real-time fluorescence quantitative polymerase chain reaction (PCR) with specific primers (forward: GGGAGCAAACAGGATTA GATACCT; reverse: TGCACCATCTGTCACTCTGTAACTC) on

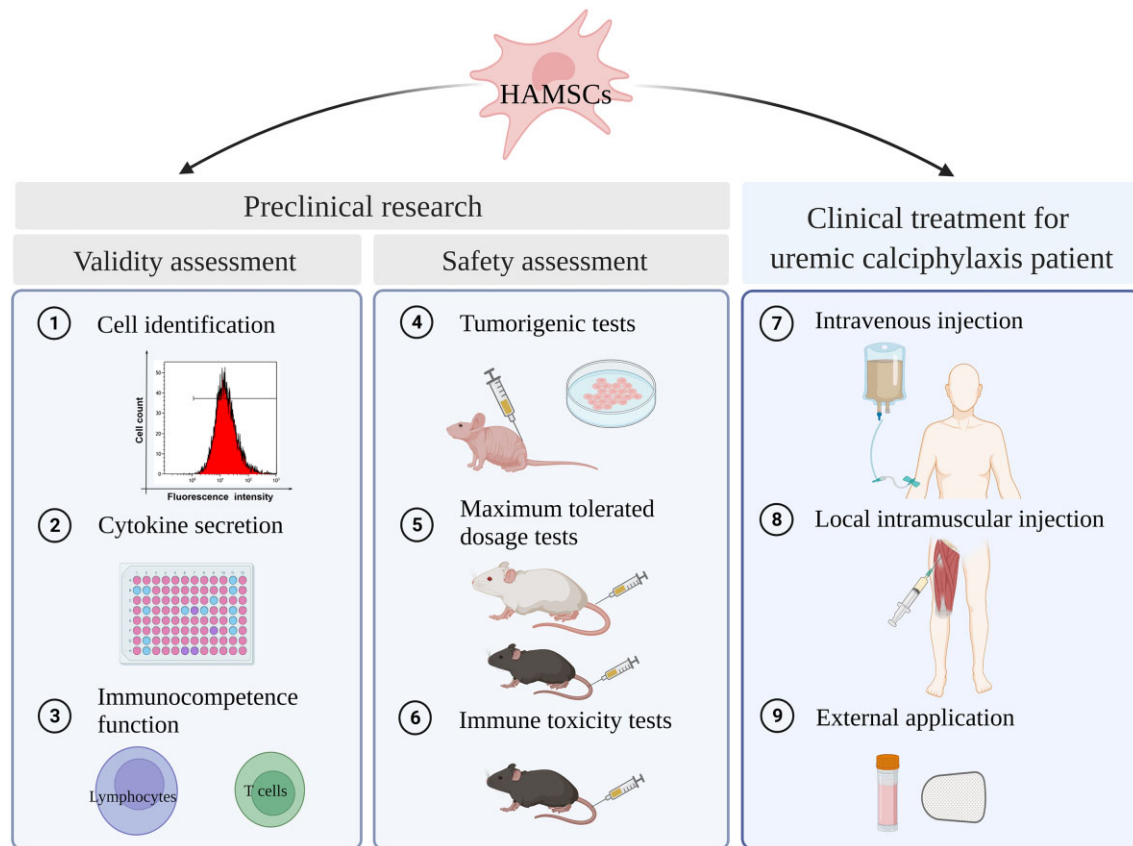


**Figure 8** Preclinical research of hAMSCs and regenerative treatment for the uremic calciphylaxis patient. Created with BioRender.com.

the QuantStudio™ 7 Flex Real-Time PCR System (Applied Biosystem®). Cell viability was assessed by living cell counting. Cell population doubling time was calculated based on living cell counting and the equation  $T_D = (t \times \log 2) / (\log N_t - \log N_0)$  ( $t$ : cell culturing time;  $N_0$ : cell number at the time of planting;  $N_t$ : cell number after  $t$ -h growing).

#### Analysis for surface markers of hAMSCs

Cells that reached 80%–90% confluence were digested with TrypLE™ (Gibco), washed with PBS, and divided into  $1 \times 10^5/10 \mu\text{l}/\text{tube}$ . The target antibodies (Supplementary Table S2) were added, placed at room temperature for 20 min, and protected from light. The cells were washed with Dulbecco's PBS (GIBCO), resuspended, transferred to a flow tube, and tested on the machine (Gallios, Beckman Coulter).

#### Analysis for cytokine secretions from hAMSC supernatants

When hAMSCs reached 80%–90% confluence *in vitro*, the culture supernatants were analyzed by enzyme-linked immunosorbent assay (ELISA). Kits from Fcmacs Biotech Co., Ltd, were applied to detect the levels of HGF, BDNF, IL-6, and IFN- $\gamma$ . VEGF, Ang-1, FGF-7, and IL-12 were measured with kits from Multisciences Biotech Co., Ltd.

#### Analysis of hAMSC immunocompetence *in vitro*

PBMCs were isolated from whole blood of a healthy control/patient and cocultured with hAMSCs at 10:1 for 72 h. Then, brefeldin A (BioLegend) was added and cells were collected after 5 h. Total lymphocytes were labelled with anti-human CD3 and CD8 antibodies (BioLegend), and Th1, Th2, and Th17 cells were labelled with anti-human CD3, CD8, IL-4, IFN- $\gamma$ , and IL-17A antibodies, respectively (BioLegend). Treg cells were labelled with anti-human CD4, CD25, and forkhead box O3 (FOXP3) antibodies (BioLegend). All cells were detected by flow cytometry.

#### hAMSC tumorigenicity assessed by soft agar experiment *in vitro*

hAMSCs (AMSC10.2.2, P5) were inoculated into soft agar (6-well plates) at low ( $1.5 \times 10^3/\text{well}$ ), medium ( $3 \times 10^3/\text{well}$ ), and high ( $6 \times 10^3/\text{well}$ ) concentrations ( $n = 3$  in each group). Human normal embryo lung fibroblasts (MRC-5, negative control) and human cervical cancer cells (Hela, positive control) were inoculated into soft agar at  $3 \times 10^3/\text{well}$ . Cells were cultured in a 37°C, 5% CO<sub>2</sub> incubator for 3 weeks, the number of colonies was counted with >20 cells in each group, and the colony formation rate was calculated.

#### Tumorigenicity tests of hAMSCs in Balbc-nu mice

Balbc-nu mice at 5–6 weeks old were subjected to tumorigenicity tests by subcutaneous inoculation of hAMSCs

( $1 \times 10^7$  cells) at one scapula area ( $n = 10$ ). The HPF5.2 cell line (prepuce fibroblasts) was established from donated prepuce tissue of a 6-year-old boy who underwent the excision of prepuce surgery, which was approved by the Ethics Committee of The First Affiliated Hospital of Nanjing Medical University, Jiangsu Province Hospital (2012-SR-128). In Balbc-nu mice, HPF5.2 cells were injected as negative control ( $n = 10$ ) and human lung cancer cells (NCI-H460 cell line) were injected as positive control ( $n = 10$ ). The mice were observed for 16 weeks and sacrificed when the tumor volume reached  $3000 \text{ mm}^3$ .

#### *The karyotype and STR analysis*

Chromosomes were visualized by Giemsa staining. A minimum of 50 metaphase hAMSCs per sample were selected to perform a full karyotype analysis (Catalina et al., 2007, 2008). Chromosome DNAs were extracted from hAMSCs, and multiplex PCR was performed for STR regions of interest (Baine and Hui, 2019). Twenty loci and amelogenin for sex determination were tested.

#### *Acute toxicity tests of single hAMSC intravenous administration in mice and rats*

C57BL/6 mice (6–8 weeks old,  $n = 10$  in each group) were injected with hAMSCs via tail vein. A total of eight dosages (equivalent to 2–32 times the clinical dosage with  $2 \times 10^6$  to  $32 \times 10^6$  cells/kg in humans) were tested. SD rats (6–12 weeks old,  $n = 4$  in each group) were injected with a total of nine dosages (equivalent to 7–53 times the clinical dosage with  $7 \times 10^6$  to  $53 \times 10^6$  cells/kg in humans). The survival time was observed for 14 days.

#### *Long-term toxicity tests of multiple hAMSC intravenous administration in mice and rats*

C57BL/6 mice (7–8 weeks old,  $n = 10$  in each group) and SD rats (9–10 weeks old,  $n = 12$  in each group) were injected with hAMSCs via tail vein every 5 days for 6 times. They had a 4-week recovery period after the final hAMSC administration.

#### *Immune toxicity tests in mice with hAMSC intravenous administration*

C57BL/6 mice (7–8 weeks old, 16–20 g for females and 18–21 g for males) were randomly divided into the control group (1% human serum albumin), hAMSC low-dosage group ( $2.5 \times 10^7$  cells/kg), hAMSC medium-dosage group ( $5.0 \times 10^7$  cells/kg), and hAMSC high-dosage group ( $1.0 \times 10^8$  cells/kg). There were 10 mice in each group, with equal numbers of female and male. The hAMSCs were administered by tail vein and repeated every 5 days for a total of three times. After 4-week recovery following the last administration, serum IgG, IgE, and IgM levels were detected by ELISA (Fcmacs Biotech Co., Ltd).

#### *Measurement of blood parameters for the uremic calciphylaxis patient*

Venous whole blood samples were drawn in the morning from the patient after overnight fasting. Routine blood tests were

performed using an LH-750 Hematology Analyzer (Beckman Coulter). Biochemical indices were measured using an automatic biochemical analyzer (AU5400; Olympus). Serum iPTH levels were measured with the second-generation iPTH assay kits by UniCel DxI800 Access Immunoassay System (Beckman Coulter). Serum tumor parameters were measured with the Cobas e602 electrochemiluminescent immunoassay instrument (Roche).

#### *Skin histopathological analysis for the calciphylaxis patient during hAMSC treatment*

H&E sections of the patient's thigh skin at different time points (before, 1 month after, and 20 months after hAMSC treatment) were investigated by light microscopy. The blood vessels were recorded at low magnification ( $100\times$ ), while inflammatory cells, including neutrophils, lymphocytes, and plasmocytes, were counted at high magnification ( $400\times$ ). Each value was determined as the mean of three microscopic vision fields selected by three experienced medical practitioners.

#### *The ethical issues of the study*

Human amniotic membranes were donated by healthy pregnant women in their 20s or 30s who underwent C-sections for full-term pregnancies and provided written informed consent, which was approved by the Ethics Committee of The First Affiliated Hospital of Nanjing Medical University, Jiangsu Province Hospital (2012-SR-128). The animal experiments were approved by the Ethics Committee of Nanjing Medical University (IACUC-1808004). Because of the rapid progression of calciphylaxis refractory to conventional therapies, the patient received hAMSC treatment, which was approved by the Ethics Committee of The First Affiliated Hospital of Nanjing Medical University, Jiangsu Province Hospital (2018-QT-001), and written informed consent was signed prior to treatment.

#### *Statistical analysis*

Continuous variables were expressed as mean  $\pm$  standard deviation. The Mech formula (expressed as  $S = KW^{2/3}$ ) was used for the dosage conversion between mice/rats and humans. The Kruskal–Wallis test and Fisher's exact test were used to analyze the relationships among control, low-dosage, medium-dosage, and high-dosage groups. A paired-sample *t*-test was used to compare blood parameters before and after hAMSC treatment.

The data were analyzed by SPSS 25.0 (SPSS Company). A two-sided *P*-value  $< 0.05$  was considered statistically significant.

#### **Supplementary material**

Supplementary material is available at *Journal of Molecular Cell Biology* online.

#### **Acknowledgements**

The authors thank the patient, her family, and clinicians who assisted with the data collection. The study was supported by the International Society of Nephrology (ISN) Mentorship Program and the authors thank Professor Marcello Tonelli

(University of Calgary, Canada) for his helpful comments and revision on the draft of the manuscript.

### Funding

This work was funded by the National Natural Science Foundation of China (81270408, 81570666, 81730041, and 81671447), the International Society of Nephrology (ISN) Clinical Research Program (18-01-0247), Construction Program of Jiangsu Provincial Clinical Research Center Support System (BL2014084), Jiangsu Province Key Medical Personnel Project (ZDRCA2016002), CKD Anemia Research Foundation from China International Medical Foundation (Z-2017-24-2037), Outstanding Young and Middle-Aged Talents Support Program of The First Affiliated Hospital of Nanjing Medical University (Jiangsu Province Hospital), the National Key Research and Development Program of China (2017YFC1001303), the Program of Jiangsu Province Clinical Medical Center (YXZXB2016001, BL2012009), the State Key Laboratory of Reproductive Medicine Program (SKLRM-GC201803), and the Program of Jiangsu Commission of Health (H201605).

**Conflict of interest:** none declared.

**Author contributions:** project conceived and directed, hAMSC clinical treatment design, and research funding support by J.L., L.Q., and N.W.; research ethical issues and administrative guidance by X.W. and N.L.; hAMSC research platform management and quality control by J.L. and L.Q.; hAMSC preparation, cell line construction, quality control, and preclinical study by L.Q., Y.C., C.J., S.N., Jing Zhou, A.C., Jie Wang, M.C., and Q.C.; human amniotic donor screening and amniotic donation by M.W., X.M., and L.C.; clinical management and multidisciplinary team rescue of the patient by N.W., K.L., F.X., Yanggang Yuan, M.Z., G.Y., J.G., Q.W., B.S., Y.G., C.O., Xueqiang Xu, Jing Wang, Y.H., H.C., Y.L., J.S., W.L., L.D., Yinbing Pan, X.L., H.W., Yanyan Pan, L.W., Xianrong Xu, and Jing Zhao; clinical guidance by C.X.; follow-up study by N.W., Jing Zhang, Y.X., F.X., and W.R.; clinical specimen collection, measurement, and data acquisition by K.L., F.X., Jing Zhang, Y.C., W.R., D.W., B.Z., X.G., Z.G., F.C., Youjia Yu, Q.J., Zhiwei Zhang, M.G., X.Z., and C.L.; analysis and interpretation of the data and writing and revision of the manuscript by N.W., L.Q., Jing Zhang, Y.X., K.L., Zhihong Zhang, Z.S., Y.L., H.Q., A.B., X.Y., F.X., W.R., F.L., S.T., J.D., and Q.W.

### References

- Alviano, F., Fossati, V., Marchionni, C., et al. (2007). Term amniotic membrane is a high throughput source for multipotent mesenchymal stem cells with the ability to differentiate into endothelial cells in vitro. *BMC Dev. Biol.* 7, 11.
- Baine, I., and Hui, P. (2019). Practical applications of DNA genotyping in diagnostic pathology. *Expert Rev. Mol. Diagn.* 19, 175–188.
- Barrientos, S., Stojadinovic, O., Golinko, M.S., et al. (2008). Growth factors and cytokines in wound healing. *Wound Repair Regen.* 16, 585–601.
- Bien, M.Y., Wu, M.P., Chen, W.L., et al. (2015). VEGF correlates with inflammation and fibrosis in tuberculous pleural effusion. *Sci. World J.* 2015, 417124.
- Brandenburg, V.M., Kramann, R., Rothe, H., et al. (2017). Calcific uraemic arteriopathy (calciphylaxis): data from a large nationwide registry. *Nephrol. Dial. Transplant.* 32, 126–132.
- Cañedo-Dorantes, L., and Cañedo-Ayala, M. (2019). Skin acute wound healing: a comprehensive review. *Int. J. Inflamm.* 2019, 3706315.
- Catalina, P., Cobo, F., Cortés, J.L., et al. (2007). Conventional and molecular cytogenetic diagnostic methods in stem cell research: a concise review. *Cell Biol. Int.* 31, 861–869.
- Catalina, P., Montes, R., Ligeró, G., et al. (2008). Human ESCs predisposition to karyotypic instability: is a matter of culture adaptation or differential vulnerability among hESC lines due to inherent properties? *Mol. Cancer* 7, 76.
- Chi, Y., Di, Q., Han, G., et al. (2019). Mir-29b mediates the regulation of Nrf2 on airway epithelial remodeling and Th1/Th2 differentiation in COPD rats. *Saudi J. Biol. Sci.* 26, 1915–1921.
- Ertl, J., Pichlsberger, M., Tuca, A.C., et al. (2018). Comparative study of regenerative effects of mesenchymal stem cells derived from placental amnion, chorion and umbilical cord on dermal wounds. *Placenta* 65, 37–46.
- Fan, Y., Ye, J., Shen, F., et al. (2008). Interleukin-6 stimulates circulating blood-derived endothelial progenitor cell angiogenesis in vitro. *J. Cereb. Blood Flow Metab.* 28, 90–98.
- Gao, S., Chen, T., Hao, Y., et al. (2020). Exosomal miR-135a derived from human amnion mesenchymal stem cells promotes cutaneous wound healing in rats and fibroblast migration by directly inhibiting LATS2 expression. *Stem Cell Res. Ther.* 11, 56.
- Guiding Principle for Cell Therapy Products Research and Assessment Technique. (2017). National Medical Products Administration of the People's Republic of China.
- Guiding Principle for Stem Cell-based Medicinal Products Quality Control and Pre-clinical Research. (2015). National Health Commission of the People's Republic of China and National Medical Products Administration of the People's Republic of China.
- Guo, Y., Bao, S., Guo, W., et al. (2019). Bone marrow mesenchymal stem cell-derived exosomes alleviate high phosphorus-induced vascular smooth muscle cells calcification by modifying microRNA profiles. *Funct. Integr. Genomics* 19, 633–643.
- Halade, G.V., Ma, Y., Ramirez, T.A., et al. (2013). Reduced BDNF attenuates inflammation and angiogenesis to improve survival and cardiac function following myocardial infarction in mice. *Am. J. Physiol. Heart Circ. Physiol.* 305, H1830–H1842.
- Harrell, C.R., Markovic, B.S., Fellabaum, C., et al. (2020). The role of interleukin 1 receptor antagonist in mesenchymal stem cell-based tissue repair and regeneration. *Biofactors* 46, 263–275.
- Hassanshahi, A., Hassanshahi, M., Khabbazi, S., et al. (2019). Adipose-derived stem cells for wound healing. *J. Cell. Physiol.* 234, 7903–7914.
- Hu, W.H., Wang, H.Y., Kong, X.P., et al. (2019). Polydatin suppresses VEGF-induced angiogenesis through binding with VEGF and inhibiting its receptor signaling. *FASEB J.* 33, 532–544.
- Iwamoto, U., Hori, H., Takami, Y., et al. (2015). A novel cell-containing device for regenerative medicine: biodegradable nonwoven filters with peripheral blood cells promote wound healing. *J. Artif. Organs* 18, 315–321.
- Jiao, D., Wang, J., Lu, W., et al. (2016a). Curcumin inhibited HGF-induced EMT and angiogenesis through regulating c-Met dependent PI3K/Akt/mTOR signaling pathways in lung cancer. *Mol. Ther. Oncolytics* 3, 16018.
- Jiao, H., Shi, K., Zhang, W., et al. (2016b). Therapeutic potential of human amniotic membrane-derived mesenchymal stem cells in APP transgenic mice. *Oncol. Lett.* 12, 1877–1883.
- Kao, H.K., Chen, B., Murphy, G.F., et al. (2011). Peripheral blood fibrocytes: enhancement of wound healing by cell proliferation, re-epithelialization, contraction, and angiogenesis. *Ann. Surg.* 254, 1066–1074.
- KDIGO Clinical Practice Guideline for Anemia in Chronic Kidney Disease. (2012). Chapter 1: diagnosis and evaluation of anemia in CKD. *Kidney Int. Suppl.* 2, 288–291.

- Kidney Disease: Improving Global Outcomes (KDIGO) CKD–MBD Update Work Group. (2017). KDIGO 2017 clinical practice guideline update for the diagnosis, evaluation, prevention, and treatment of chronic kidney disease–mineral and bone disorder (CKD–MBD). *Kidney Int. Suppl.* 7, 1–59.
- Li, J.Y., Ren, K.K., Zhang, W.J., et al. (2019). Human amniotic mesenchymal stem cells and their paracrine factors promote wound healing by inhibiting heat stress-induced skin cell apoptosis and enhancing their proliferation through activating PI3K/AKT signaling pathway. *Stem Cell Res. Ther.* 10, 247.
- Liu, H., Jiang, C., La, B., et al. (2021b). Human amnion-derived mesenchymal stem cells improved the reproductive function of age-related diminished ovarian reserve in mice through Ampk/FoxO3a signaling pathway. *Stem Cell Res. Ther.* 12, 317.
- Liu, Y., Bao, S., Guo, W., et al. (2021a). Bone mesenchymal stem cell derived exosomes alleviate high phosphorus-induced calcification of vascular smooth muscle cells through the NONHSAT 084969.2/NF- $\kappa$ B axis. *Aging* 13, 16749–16762.
- Maraldi, T., Beretti, F., Guida, M., et al. (2015). Role of hepatocyte growth factor in the immunomodulation potential of amniotic fluid stem cells. *Stem Cells Transl. Med.* 4, 539–547.
- McCarthy, J.T., El-Azhary, R.A., Patzelt, M.T., et al. (2016). Survival, risk factors, and effect of treatment in 101 patients with calciphylaxis. *Mayo Clin. Proc.* 91, 1384–1394.
- Meeh, K. (1879). Oberflächenmessungen des menschlichen körpers und seine einzelnen teile in den verschiedenen altersstufen. *Z. F. Biol.* 15, 425–458.
- Mishra, V.K., Shih, H.H., Parveen, F., et al. (2020). Identifying the therapeutic significance of mesenchymal stem cells. *Cells* 9, 1145.
- Nair, A., Morsy, M.A., and Jacob, S. (2018). Dose translation between laboratory animals and human in preclinical and clinical phases of drug development. *Drug Dev. Res.* 79, 373–382.
- Nair, A.B., and Jacob, S. (2016). A simple practice guide for dose conversion between animals and human. *J. Basic Clin. Pharm.* 7, 27–31.
- Nigwekar, S.U., Thadhani, R., and Brandenburg, V.M. (2018). Calciphylaxis. *N. Engl. J. Med.* 378, 1704–1714.
- Pang, Y., Liang, M.T., Gong, Y., et al. (2018). HGF reduces disease severity and inflammation by attenuating the NF- $\kappa$ B signaling in a rat model of pulmonary artery hypertension. *Inflammation* 41, 924–931.
- Pedersen, B.K. (2013). Muscle as a secretory organ. *Compr. Physiol.* 3, 1337–1362.
- Peng, T., Zhuo, L., Wang, Y., et al. (2018). Systematic review of sodium thiosulfate in treating calciphylaxis in chronic kidney disease patients. *Nephrology* 23, 669–675.
- Potente, M., Gerhardt, H., and Carmeliet, P. (2011). Basic and therapeutic aspects of angiogenesis. *Cell* 146, 873–887.
- Qu, Y., Cao, C., Wu, Q., et al. (2018). The dual delivery of KGF and bFGF by collagen membrane to promote skin wound healing. *J. Tissue Eng. Regen. Med.* 12, 1508–1518.
- Seethapathy, H., and Nigwekar, S.U. (2019). Revisiting therapeutic options for calciphylaxis. *Curr. Opin. Nephrol. Hypertens.* 28, 448–454.
- Shi, C.S., Wang, D.L., Sun, J., et al. (2020). Influence of human amniotic mesenchymal stem cells on macrophage phenotypes and inflammatory factors in full-thickness skin wounds of mice. *Zhonghua Shao Shang Za Zhi* 36, 288–296.
- Shi, Y., Wang, Y., Li, Q., et al. (2018). Immunoregulatory mechanisms of mesenchymal stem and stromal cells in inflammatory diseases. *Nat. Rev. Nephrol.* 14, 493–507.
- Sun, H., Hou, Z., Yang, H., et al. (2014). Multiple systemic transplantations of human amniotic mesenchymal stem cells exert therapeutic effects in an ALS mouse model. *Cell Tissue Res.* 357, 571–582.
- Topoluk, N., Hawkins, R., Tokish, J., et al. (2017). Amniotic mesenchymal stromal cells exhibit preferential osteogenic and chondrogenic differentiation and enhanced matrix production compared with adipose mesenchymal stromal cells. *Am. J. Sports Med.* 45, 2637–2646.
- Tvedt, T.H.A., Ersvaer, E., Tveita, A.A., et al. (2017). Interleukin-6 in allogeneic stem cell transplantation: its possible importance for immunoregulation and as a therapeutic target. *Front. Immunol.* 8, 667.
- Waldner, M.J., Wirtz, S., Jefremow, A., et al. (2010). VEGF receptor signaling links inflammation and tumorigenesis in colitis-associated cancer. *J. Exp. Med.* 207, 2855–2868.
- Wang, Y., Li, L., Guo, X., et al. (2012). Interleukin-6 signaling regulates anchorage-independent growth, proliferation, adhesion and invasion in human ovarian cancer cells. *Cytokine* 59, 228–236.
- Wang, L., Zhang, X., Liu, X., et al. (2019). Overexpression of  $\alpha$ 5 $\beta$ 1 integrin and angiopoietin-1 co-operatively promote blood–brain barrier integrity and angiogenesis following ischemic stroke. *Exp. Neurol.* 321, 113042.
- Wei, W., Guo, X., Gu, L., et al. (2021). Bone marrow mesenchymal stem cell exosomes suppress phosphate-induced aortic calcification via SIRT6–HMGB1 deacetylation. *Stem Cell Res. Ther.* 12, 235.
- Zhang, D., Yan, K., Zhou, J., et al. (2019). Myogenic differentiation of human amniotic mesenchymal cells and its tissue repair capacity on volumetric muscle loss. *J. Tissue Eng.* 10, 2041731419887100.
- Zhao, J., Li, Q., Muktiali, M., et al. (2020). Effect of microwave ablation treatment of hepatic malignancies on serum cytokine levels. *BMC Cancer* 20, 812.
- Zhao, L., Johnson, T., and Liu, D. (2017). Therapeutic angiogenesis of adipose-derived stem cells for ischemic diseases. *Stem Cell Res. Ther.* 8, 125.
- Zhou, Z.F., Peng, F., Li, J.Y., et al. (2019). Intratumoral IL-12 gene therapy inhibits tumor growth in a HCC–hu–PBL–NOD/SCID murine model. *Oncotargets Ther.* 12, 7773–7784.